

Performance Analysis of Cooperative Systems with Unreliable Backhauls and Selection Combining

Kim, K.J.; Khan, T.; Orlik, P.V.

TR2016-149 June 2016

Abstract

In this paper, a cooperative wireless system with unreliable wireless backhaul connections is investigated. To increase the throughput and maximize the receiver signal-to-noise ratio (SNR), a selection combining protocol is employed. Each transmitter is connected to the control unit via independent but unreliable wireless backhaul connections. Simultaneously taking into account the reliability of each backhaul and different fading conditions of Nakagami- m fading channels, the statistical properties of the effective-SNR at the receiver are investigated. Closed-form expressions are derived for several performance metrics including the outage probability, average spectral efficiency, and average symbol error rate. The effects of backhaul reliability on these performance metrics are also investigated. The scaling relationship between the convergence behavior of these performance metrics and the conventional diversity gain is also analytically investigated in the asymptotic high SNR regime. Monte-Carlo simulations are conducted to verify the derived impact of backhaul reliability on the performance.

IEEE Transactions on Vehicular Technology

This work may not be copied or reproduced in whole or in part for any commercial purpose. Permission to copy in whole or in part without payment of fee is granted for nonprofit educational and research purposes provided that all such whole or partial copies include the following: a notice that such copying is by permission of Mitsubishi Electric Research Laboratories, Inc.; an acknowledgment of the authors and individual contributions to the work; and all applicable portions of the copyright notice. Copying, reproduction, or republishing for any other purpose shall require a license with payment of fee to Mitsubishi Electric Research Laboratories, Inc. All rights reserved.

Performance Analysis of Cooperative Systems with Unreliable Backhauls and Selection Combining

Kyeong Jin Kim, *Senior Member, IEEE*, Talha Ahmed Khan, *Student Member, IEEE*, and Philip Orlik, *Senior Member, IEEE*

Abstract—In this paper, a cooperative wireless system with unreliable wireless backhaul connections is investigated. To increase the throughput and maximize the receiver signal-to-noise ratio (SNR), a selection combining protocol is employed. Each transmitter is connected to the control unit via independent but unreliable wireless backhaul connections. Simultaneously taking into account the reliability of each backhaul and different fading conditions of Nakagami- m fading channels, the statistical properties of the effective-SNR at the receiver are investigated. Closed-form expressions are derived for several performance metrics including the outage probability, average spectral efficiency, and average symbol error rate. The effects of backhaul reliability on these performance metrics are also investigated. The scaling relationship between the convergence behavior of these performance metrics and the conventional diversity gain is also analytically investigated in the asymptotic high SNR regime. Monte-Carlo simulations are conducted to verify the derived impact of backhaul reliability on the performance.

Index Terms—Wireless backhaul, backhaul reliability, selection combining protocol, outage probability, average spectral efficiency, average symbol error rate, scaling law, Nakagami- m fading.

I. INTRODUCTION

DRIVEN by data-intensive applications and emerging paradigms such as smart cities and the Internet of Things, wireless traffic volume is predicted to show an exponential growth [1]. To meet the growing traffic demands, future wireless network deployments are expected to get more dense and heterogeneous [2]. With such a large-scale access point (AP) deployment, the backhaul links connecting the APs to the network backbone (or cloud) are also expected to get more dense. In traditional networks, the backhaul infrastructure has typically consisted of highly reliable wired (or fiber) links. It seems less likely, though, that this *wired* backhaul infrastructure could be expanded to support future networks. This can be attributed to the excessive capital injection required for sustaining such a large-scale backhaul deployment, and to topology and access-related issues [3], [4]. This leaves wireless backhaul as a suitable alternative for the dense networks of the future. The information exchanged over the backhauls,

however, will now be intrinsically unreliable due to wireless nature of the communication channel.

Recently, the investigation of unreliable and heterogeneous backhauls has attracted considerable interest in the area of the coordinated multi-point (CoMP) cooperation. The impact of unreliable backhaul links on the average sum rate for a CoMP system has been investigated in [3]. While prior work typically uses the outage probability and spectral efficiency as performance metrics, the impact of unreliable backhaul on the delay performance of a heterogeneous cellular network has also been investigated [5]. Another line of work studies the impact of a finite-capacity backhaul on the system performance. For the uplink of a cloud radio access network, it has been shown that the capacity of the backhaul connection is one of the key parameters that affect the sum-rate performance [6]. A game-theoretic approach is used to investigate the impact of heterogeneous backhauls on the coherent downlink CoMP cooperation in femtocells assuming highly reliable wired and wireless backhauls [7]. It is shown that unreliable backhauls can significantly limit the performance gains promised by the CoMP cooperation.

While there are many preexisting studies that investigate the impact of unreliable backhauls for CoMP based cellular networks, we mainly focus on non-cellular systems in this paper. Several papers considering non-cellular systems can be found in the open literature. For example, in [8], the authors investigate broadcast coding and distributed source coding techniques including distributed compression for a cooperative relay network with unreliable backhaul connections between the relay and the destination. For a finite-sized network under Nakagami- m fading, [9] provides an analytical outage probability without transmitter cooperation. For an arbitrarily shaped finite-sized wireless network, [10] investigates the outage probability of the non-cooperative system with perfect backhauls. For a finite backhaul capacity, data sharing is proposed for the uplink cooperation in [11]. For two source nodes connected by orthogonal limited-rate error free backhauls, the outer bound on the capacity region for multicast relaying is derived in [12]. In [13], the authors investigate cooperative network coding for relay-assisted two sources and two destinations networks assuming an ideal backhaul connection between the source nodes. For the uplink one-way and two-hop relaying network, a network precoding is proposed in [14] to increase the throughput while achieving the full diversity. In [3], the authors define an equivalent channel matrix based on the link failure probability (LFP) and investigate the impact of the backhaul LFP on the empirical ergodic capacity. In [15],

Manuscript received April 29, 2015; revised November 6, 2015, March 25, 2016, and June 9, 2016; accepted June 20, 2016. The editor coordinating the review of this paper and approving it for publication was Dr. D. Marabissi.

K. J. Kim and P. V. Orlik are with Mitsubishi Electric Research Laboratories (MERL), Cambridge, MA 02139 USA (e-mail: kyeong.j.kim@hotmail.com).

T. A. Khan was with Mitsubishi Electric Research Laboratories (MERL), Cambridge, MA 02139 USA. He is now with the Department of Electrical and Computer Engineering, University of Texas at Austin, Austin, TX 78712 USA.

a distributed precoder is designed based on the channel state information (CSI), which is impaired by backhaul latency and limited capacity.

In this paper, to model the fading characteristics, we assume Nakagami- m fading channels with different fading parameters, and focus on investigating the impact of unreliable backhaul on the performance of selection combining (SC)-assisted [16]–[19] cooperative systems. In contrast to the preexisting work, our main contributions are summarized as follows.

- We employ a Bernoulli process to model backhaul reliability¹ in the proposed system; that is, we take into account successful and failed reception of the common message between the control unit (CU) and the transmitters.
- Considering the receiver complexity and signaling overhead, we employ the SC protocol [16]–[19] at the receiver to select the maximum effective signal-to-noise ratio (e-SNR) across all the received signals from the CU to the receiver to achieve diversity gain without requiring CSI at the transmitters. For this system, we define the e-SNR² motivated by the work in [9], [10], and [17], which is the product of the Bernoulli random process that models backhaul reliability and the Nakagami- m random process that models a fading channel from the transmitter to the receiver. Different Nakagami- m m parameters³ are used to model different fading conditions across the nodes in the system as in [9] and [27]. However, unlike [9] and [27], the impact of the backhaul reliability on the performance has been investigated in this paper, which is one of the novel contributions. Based on the statistical properties of the e-SNR, we derive the outage probability, average spectral efficiency (ASE), and average symbol error rate (ASER).
- Analytical performance analysis provides insights into the scaling behavior of the considered performance metrics in the asymptotic high SNR regime. Our findings show that the rate of convergence to the asymptotic limit is determined by the degrees of transmitter cooperation and the Nakagami- m m parameter. We also confirm that lower bounds on the outage probability and ASER are exclusively determined by a set of backhaul reliability levels.

Organization: The rest of the paper is organized as follows. In Section II, we first detail the system and channel model of the proposed system. Performance analysis of the considered system is presented in Section III. Simulation results are presented in Section IV and conclusions are drawn in Section V.

¹Reliability is the capability of a system to execute required tasks within certain constraints. It is measured as a probability that the proposed system can perform its functions without error within a specific time period [20]. Thus, the *backhaul reliability* [21] is used to model a successful delivery of the message which allows participation in the cooperative transmission.

²Note that the e-SNR is widely used in the SC protocol [16], [17], opportunistic scheduling [22], [23], partial best relay selection (PBRs) [24], [25], and best relay selection [26].

³For analytical analysis convenience, we limit to the case of Nakagami- m fading with a positive integer value of m .

Notation: $\mathcal{CN}(\mu, \sigma^2)$ denotes the complex Gaussian distribution with the mean μ and the variance σ_n^2 ; $F_\varphi(\cdot)$ and $f_\varphi(\cdot)$, respectively, denote the cumulative distribution function (CDF) and probability density function (PDF) of the random variable (RV) φ ; $E\{\cdot\}$ denotes the expectation. Additional notation used in this paper is summarized in Table 1.

TABLE I
NOTATION USED IN THIS PAPER

Notation	Description
$O_{\text{out}}(\theta)$	Outage probability of the cooperative system with unreliable backhauls at outage threshold θ
$O_{\text{out}}^1(\theta)$	Outage probability of the non-cooperative system with unreliable backhauls at outage threshold θ
$O_{\text{out}}^{K,R}(\theta)$	Outage probability of the cooperative system in Rayleigh fading with unreliable backhauls at outage threshold θ
$O_{\text{out}}^c(\theta)$	Outage probability of the cooperative system with completely reliable backhauls at outage threshold θ
$O_{\text{out}}^{1,c}(\theta)$	Outage probability of the non-cooperative system with completely reliable backhauls at outage threshold θ
$O_{\text{out}}^{\text{as},c}(\theta)$	Asymptotic outage probability of the cooperative system with completely reliable backhauls at outage threshold θ
$O_{\text{out}}^{\text{as}}(\theta)$	Asymptotic outage probability of the cooperative system with unreliable backhauls at outage threshold θ
$O_{\text{out}}^{\text{MRT}}(\theta)$	Outage probability of the cooperative system with unreliable backhauls and MRT at outage threshold θ
$O_{\text{out}}^{c,\text{MRT}}(\theta)$	Outage probability of the cooperative system with completely reliable backhauls and MRT at outage threshold θ
$O_{\text{out}}^{\text{as},\text{MRT}}(\theta)$	Asymptotic outage probability of the cooperative system with unreliable backhauls and MRT at outage threshold θ
R	Average spectral efficiency of the cooperative system with unreliable backhauls
R^1	Average spectral efficiency of the non-cooperative system with unreliable backhauls
$R^{K,R}$	Average spectral efficiency of the cooperative system in Rayleigh fading with unreliable backhauls
R^c	Average spectral efficiency of the cooperative system with completely reliable backhauls
R^{as}	Asymptotic spectral efficiency of the cooperative system with unreliable backhauls
R^{MRT}	Average spectral efficiency of the cooperative system with unreliable backhauls and MRT
$S(e)$	Average symbol error rate with unreliable backhauls
$S^c(e)$	Average symbol error rate with completely reliable backhauls
$S^{\text{as}}(e)$	Asymptotic average symbol error rate with unreliable backhauls
$S^{\text{MRT}}(e)$	Average symbol error rate with unreliable backhauls and MRT
$S^{\text{as},\text{MRT}}(e)$	Asymptotic average symbol error rate with unreliable backhauls and MRT

Laplace transform of the Meijer G-function: Since the Laplace transform of a particular Meijer G-function [28, eq. (07.34.22.0003.01)], [29, eq. (2.24.3.1)] is repeatedly used in this paper, we summarize it in the following equation:

$$(s)^{-\alpha} G_{p+1,q}^{m,n+1} \left(\frac{a}{s} \middle| \begin{matrix} 1-\alpha, a_1, \dots, a_n, a_{n+1}, \dots, a_p \\ b_1, \dots, b_m, b_{m+1}, \dots, b_q \end{matrix} \right) = \int_0^\infty t^{\alpha-1} e^{-st} G_{p,q}^{m,n} \left(at \middle| \begin{matrix} a_1, \dots, a_n, a_{n+1}, \dots, a_p \\ b_1, \dots, b_m, b_{m+1}, \dots, b_q \end{matrix} \right) dt \quad (1)$$

where $G_{p,q}^{m,n} \left(t \middle| \begin{matrix} a_1, \dots, a_n, a_{n+1}, \dots, a_p \\ b_1, \dots, b_m, b_{m+1}, \dots, b_q \end{matrix} \right)$ denotes the Meijer G-function [30, eq. (9.301)].

II. SYSTEM AND CHANNEL MODEL

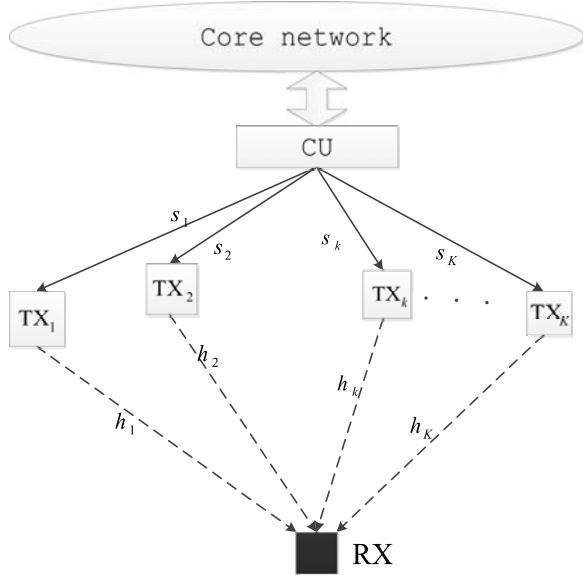


Fig. 1. Block diagram of the considered cooperative system. A CU connected to the core network provides reliable backhauls to the transmitters communicating with a receiver.

Fig. 1 shows the block diagram of the considered system consisting of a CU which is connected to the core network, and provides unreliable wireless backhauls to K transmitters communicating with a receiver (RX). The k th transmitter, TX_k , is connected with the receiver via a wireless channel h_k . All the transmitters and the receiver are assumed to be equipped with a single antenna. The major assumptions are listed below starting with the channel model.

- We do not apply coding, modulation, automatic repeat request (ARQ), and power control when a backhaul transmission is not successful. However, for cooperative one shot communications, we assume that if the message does not arrive in a reasonable time through the dedicated backhaul, a transmitter refrains from transmission. Thus, the k th transmitter, TX_k , is participating in the transmission if the message is successfully delivered over its dedicated backhaul with probability s_k , whereas it defers its transmission with probability $1 - s_k$. We model the reliability of the k th backhaul [21] by using an indicator function \mathbb{I}_k with $\Pr(\mathbb{I}_k = 1) = s_k$ and $\Pr(\mathbb{I}_k = 0) = 1 - s_k$.
- Envelopes of a set of channels, $\{h_k, \forall k\}$, from K transmitters to the receiver undergo Nakagami- m fading. This assumption is fairly general and allows us to characterize a wide range of channel models with Rayleigh and Ricean as special cases. To further generalize our channel model, Nakagami- m parameters are allowed to be different across the nodes.

- By virtue of the SC protocol⁴ [16]–[19], perfect knowledge of CSI is not required at the transmitters unlike the case of the maximum ratio transmission (MRT) [31], [32].
- Signal constellations of M-ary phase-shift keying (M-PSK) and square M-ary quadrature amplitude modulation (M-QAM) are employed. Due to perfect synchronization between the transmitters, the transmission symbol x is transmitted from the transmitters simultaneously. For these considered signal constellations, we assume that $E\{x\} = 0$ and $E\{|x|^2\} = 1$.

Having applied the SC protocol, the received signal at the receiver is given by

$$y = \sqrt{P_T}(h_{k^*})(\mathbb{I}_{k^*})x + z \quad (2)$$

where

$$k^* = \arg \max_{1 \leq k \leq K} |\mathbb{I}_k h_k|^2 \quad (3)$$

is the index of the selected transmitter, P_T is the maximum transmission power at the transmitters, and $z \sim \mathcal{CN}(0, \sigma_n^2)$.

III. PERFORMANCE ANALYSIS

After defining the e-SNR, we will first investigate its statistical properties in terms of the PDF and CDF. And then, we will derive the outage probability, ASE, and ASER sequentially.

A. Derivation of the CDF of the e-SNR

From the received signal expressed by (2), the e-SNR is defined as follows:

$$\lambda = \max_{k=1, \dots, K} \left(\frac{P_T \mathbb{I}_k |h_k|^2}{\sigma_n^2} \right) \triangleq \max_{k=1, \dots, K} (\mathbb{I}_k \lambda_k) \quad (4)$$

where $\lambda_k \triangleq \frac{P_T |h_k|^2}{\sigma_n^2}$. From the Nakagami- m fading envelope for h_k , λ_k is distributed according to the gamma distribution, which is denoted by $\lambda_k \sim \text{Ga}(m_k, \eta_k)$, where m_k is the shape of the gamma distribution which controls fading severity, and $\eta_k \triangleq \frac{P_T E\{|h_k|^2\}}{m_k \sigma_n^2}$ is the scale factor which defines the average fading power [33], [34]. The operating frequency, antenna heights, polarizations, antenna separation distance, and relative position of the scatters contribute in determining the fading severity [34].

For a positive integer value of m_k , the PDF and CDF of λ_k are given, respectively, as

$$\begin{aligned} f_{\lambda_k}(x) &= \frac{1}{\Gamma(m_k)(\eta_k)^{m_k}} x^{m_k-1} e^{-\frac{x}{\eta_k}} \text{ and} \\ F_{\lambda_k}(x) &= 1 - \frac{\Gamma_u(m_k, x/\eta_k)}{\Gamma(m_k)} \end{aligned} \quad (5)$$

where $\Gamma(x) \triangleq \int_0^\infty e^{-t} t^{x-1} dt$, and the upper incomplete gamma function is defined by $\Gamma_u(m_k, x) \triangleq \int_x^\infty e^{-t} t^{m_k-1} dt$.

⁴Note that the employed SC protocol is similar to the opportunistic scheduling [22], [23], in which a single transmitter providing the maximum e-SNR is selected. To this end, the measured e-SNRs across all the channels from the CU to the receiver should be fed back to the CU. In addition, if we take into account e-SNRs over the channels from the transmitters to the receiver while choosing a single transmitter for data transmission, the employed SC protocol is similar to PBRs in the cooperative relay network [24], [25].

Based on (4), $\mathbb{I}_k \lambda_k$ is distributed as the product of the Beroulli random process for \mathbb{I}_k and a random process which has the gamma distribution with shape m_k and scale η_k . Thus, the expression for the e-SNR is different from the existing ones [33], [35]–[37] since the backhaul reliability and the SC protocol are simultaneously incorporated in the definition of the e-SNR.

Theorem 1: For independent Nakagami- m fading channel envelopes, an independent Bernoulli random process that models backhaul reliability, and the SC protocol, the CDF of the e-SNR λ is given by

$$F_\lambda(x) = 1 + \sum_{k=1}^K (-1)^k \Upsilon \prod_{t=1}^k \left(\frac{s_{q_t}}{\ell_t! (\eta_{q_t})^{\ell_t}} \right) e^{-\beta x} x^{\bar{l}} \quad (6)$$

where $\beta \triangleq \sum_{t=1}^k \frac{1}{\eta_{q_t}}$, $\bar{l} \triangleq \sum_{t=1}^k \ell_t$, and

$$\Upsilon \triangleq \sum_{q_1=1}^{K-k+1} \cdots \sum_{q_k=q_{k-1}+1}^K \sum_{\ell_1=0}^{m_{q_1}-1} \cdots \sum_{\ell_k=0}^{m_{q_k}-1}. \quad (7)$$

Proof: See Appendix A. ■

Note that this theorem provides a general distribution of the e-SNR allowing for any degrees of transmitter cooperation, non-identical backhaul reliabilities as well as non-identical Nakagami- m fading across the nodes in the system. Then, the PDF of the e-SNR λ can be immediately derived as follows:

$$f_\lambda(x) = \sum_{k=1}^K (-1)^k \Upsilon \prod_{t=1}^k \left(\frac{s_{q_t}}{\ell_t! (\eta_{q_t})^{\ell_t}} \right) \left(\bar{l} e^{-\beta x} x^{\bar{l}-1} - \beta e^{-\beta x} x^{\bar{l}} \right). \quad (8)$$

Based on the derived PDF and CDF of the e-SNR, we will investigate the impact of backhaul reliability on several performance metrics such as the outage probability, ASE, and ASER.

B. Outage Probability Analysis

To predict the quality of service of the proposed system over non-identical Nakagami- m fading channels, we first investigate the outage probability. The outage probability $O_{\text{out}}(\theta)$ for a given e-SNR threshold θ , that is, the probability that the e-SNR falls below a given threshold θ , is given by

$$O_{\text{out}}(\theta) \triangleq \Pr(\lambda \leq \theta) = F_\lambda(\theta) \quad (9)$$

so that the outage probability is the CDF of the e-SNR evaluated at θ . We specialize the outage probability for the following two cases of interest.

1) Non-Cooperative System:

Corollary 1: The outage probability of the non-cooperative system, (i.e., $K = 1$), with unreliable backhaul is given by

$$O_{\text{out}}^1(\theta) = (1 - s_1) + s_1 \frac{\gamma_l(m_1, \theta/\eta_1)}{\Gamma(m_1)} \quad (10)$$

where the lower incomplete gamma function is defined by $\gamma_l(m_k, x) \triangleq \Gamma(m_k) - \Gamma(m_k, x)$.

Proof: Using the CDF provided in (A.3), we can see that $1 - \frac{s_1 \Gamma(m_1, \theta/\eta_1)}{\Gamma(m_1)} = (1 - s_1) + s_1 \frac{\gamma_l(m_1, \theta/\eta_1)}{\Gamma(m_1)}$. ■

2) *Cooperative System in Rayleigh Fading:* The proposed cooperative system with unreliable backhubs in Rayleigh fading, $m_k = 1, \forall k$, yields the outage probability as follows:

$$O_{\text{out}}^{K,R}(\theta) = 1 + \sum_{k=1}^K (-1)^k \Phi \prod_{t=1}^k (s_t) e^{-\beta \theta} \quad (11)$$

where $\Phi \triangleq \sum_{q_1=1}^{K-k+1} \cdots \sum_{q_k=q_{k-1}+1}^K$. At a given e-SNR threshold θ , we can readily derive (11) from the CDF derived in (6).

3) *Cooperative System with Completely Reliable Backhubs:*

Corollary 2: When the backhubs are completely reliable, the outage probability of the proposed cooperative system is given by

$$O_{\text{out}}^c(\theta) = 1 + \sum_{k=1}^K (-1)^k \Upsilon \prod_{t=1}^k \left(\frac{1}{\ell_t! (\eta_{q_t})^{\ell_t}} \right) e^{-\beta \theta} (\theta)^{\bar{l}}. \quad (12)$$

Proof: From (6), we can obtain this expression by replacing s_{q_t} with $s_{q_t} = 1, \forall t$. ■

Based on this corollary, the outage probability of the non-cooperative system is given by

$$O_{\text{out}}^{1,c}(\theta) = \frac{\gamma_l(m_1, \theta/\eta_1)}{\Gamma(m_1)}. \quad (13)$$

In order to get further insights, we provide a scaling result for the asymptotic outage probability. We first derive an asymptotic outage probability expression in the following corollary for the cooperative system with completely reliable backhubs.

Corollary 3: An asymptotic outage probability of the cooperative system with completely reliable backhubs is given by

$$O_{\text{out}}^{\text{as},c}(\theta) = C_1 \left(\frac{P_T}{\sigma_n^2} \right)^{-\sum_{k=1}^K m_k} \quad (14)$$

where $C_1 \triangleq \prod_{k=1}^K \left(\frac{1}{\Gamma(m_k+1)} \left(\frac{\theta m_k}{E\{|h_k|^2\}} \right)^{m_k} \right)$. Thus, at a fixed e-SNR threshold θ , the achievable outage diversity gain is $G_d = \sum_{k=1}^K m_k$.

Proof: See Appendix B. ■

Note that Corollary 3 verifies that the degrees of transmitter cooperation and a set of Nakagami- m parameters jointly determine the overall diversity gain in the outage probability. In contrast to Corollary 3, when backhubs are unreliable, an intrinsic asymptotic outage limit exists.

Theorem 2: The asymptotic outage probability with respect to P_T/σ_n^2 as P_T/σ_n^2 goes to infinity of the system with K cooperative transmitters and with unreliable backhubs is given by

$$O_{\text{out}}^{\text{as}}(\theta) = \prod_{k=1}^K (1 - s_k) \triangleq \Lambda_K. \quad (15)$$

Proof: See Appendix C. ■

Theorem 2 verifies that Λ_K gives a performance limit on the outage probability when backhauls are unreliable and is solely a function of the backhaul reliability levels.

C. Average Spectral Efficiency Analysis

Using the derived PDF expression for the e-SNR, the closed-form expression for the ASE can be derived as follows:

$$R = E\{\log_2(1 + \lambda)\} = \frac{1}{\ln(2)} \int_0^\infty \ln(1 + x) f_\lambda(x) dx. \quad (16)$$

With some manipulations, the closed-form expression for the ASE is provided in the following theorem.

Theorem 3: The achievable ASE of the proposed cooperative system with unreliable backhauls is given in (17) at the top of the next page.

Proof: See Appendix D. ■

Theorem 3 provides the ASE of the proposed system for a wide range of scenarios with non-identical backhaul reliability and any degrees of transmitter cooperation. When the backhaul links are completely reliable, we can obtain R^c by replacing s_k with $s_k = 1, \forall k$. Next, we will investigate the ASEs for the non-cooperative system, $K = 1$, and the system in Rayleigh fading.

1) *Non-Cooperative System:* Setting $K = 1$ in (17), yields the ASE for the non-cooperative system.

$$R^1 = \frac{-s_1}{\ln(2)} \sum_{l=0}^{m_1-1} \frac{1}{\Gamma(l+1)\eta_1^l} \left(lG_{2,3}^{3,1} \left(\frac{1}{\eta_1} \middle| \begin{matrix} -l, 1-l \\ 0, -l, -l \end{matrix} \right) - \frac{1}{\eta_1} G_{2,3}^{3,1} \left(\frac{1}{\eta_1} \middle| \begin{matrix} -1-l, -l \\ 0, -1-l, -1-l \end{matrix} \right) \right). \quad (18)$$

Note that as the backhaul reliability increases, a higher ASE can be obtained. However, when the backhaul is completely unreliable, it yields $R^1 = 0$ due to $s_1 = 0$. Also, at a fixed backhaul reliability, a higher ASE can be obtained as the value of m_1 increases since signal power fluctuation decreases [38].

2) *Cooperative System in Rayleigh Fading:* In this particular scenario, we fix $m_k = 1, \forall k$. Then the ASE of the considered cooperative system with K transmitters in Rayleigh fading is given by

$$R^{K,R} = \frac{-1}{\ln(2)} \sum_{k=1}^K (-1)^k \Phi \prod_{t=1}^k (s_t) \beta G_{2,3}^{3,1} \left(\beta \middle| \begin{matrix} -1, 0 \\ 0, -1, -1 \end{matrix} \right) \quad (19)$$

which can be derived via Eqs. (1) and (11).

3) *Asymptotic Average Spectral Efficiency Analysis:* The asymptotic ASE as $P_T/\sigma_n^2 \rightarrow \infty$ is given by

$$R^{\text{as}} = \int_0^\infty \ln(x) f_\lambda(x) dx. \quad (20)$$

Substituting $f_\lambda(x)$ with (8), and using [30, eq. (4.352.1)], (20) can be evaluated as in (21) at the top of the next page.

D. Average Symbol Error Rate Analysis

We will use the CDF of the e-SNR in the derivation of the ASER. For several signal constellations including M-PSK and square M-QAM, the ASER is given by [39], [40]

$$S(e) = \int_0^\infty P_e(x|\lambda) f_\lambda(x) dx \quad (22)$$

where $P_e(x|\lambda)$ denotes the conditional symbol error rate over the e-SNR. For the considered signal constellations, it is given that $P_e(x|\lambda) = 2AQ(\sqrt{2B\lambda})^5$, where $Q(\cdot)$ denotes the Q-function, and (A, B) are, respectively, given by [39], [40]

$$(A, B) = \begin{cases} (1, \sin^2(\pi/M)), & \text{M-PSK,} \\ \left((2 - 2/\sqrt{M}), \frac{3}{2(M-1)} \right), & \text{square M-QAM.} \end{cases} \quad (23)$$

Based on this, the ASER is derived in the following theorem.

Theorem 4: For M-PSK and square M-QAM signal constellations, the ASER of the proposed cooperative system with unreliable backhauls in Nakagami- m fading is given by

$$S(e) = 1 + \frac{A\sqrt{B}}{\sqrt{2\pi}} \sum_{k=1}^K (-1)^k \Upsilon \prod_{t=1}^k \left(\frac{s_{q_t}}{\ell_t!(\eta_{q_t})^{\ell_t}} \right) \Gamma(l+1/2) (\beta + B)^{-(l+1/2)}. \quad (24)$$

Proof: See Appendix E. ■

With completely reliable backhauls, the ASER, $S^\infty(e)$ is derived as

$$S^c(e) = 1 + \frac{A\sqrt{B}}{\sqrt{2\pi}} \sum_{k=1}^K (-1)^k \Upsilon \prod_{t=1}^k \left(\frac{1}{\ell_t!(\eta_{q_t})^{\ell_t}} \right) \Gamma(l+1/2) (\beta + B)^{-(l+1/2)} \quad (25)$$

where $S^c(e)$ can be immediately obtained from $S(e)$ by replacing s_k with $s_k = 1, \forall k$, so that we recover the achievable asymptotic diversity gain from the ASER in the following corollary.

Corollary 4: The achievable diversity gain by transmitter cooperation is given by $G_{d,\text{ASER}} = \sum_{k=1}^K m_k$.

Proof: See Appendix F. ■

This corollary shows that the degrees of transmitter cooperation and a set of m values of the Nakagami- m fading jointly determine the achievable diversity gain.

Theorem 5: When unreliable backhauls are connected to the cooperative system, the diversity gain is not achievable due to the limit on the ASER. This limit is exclusively determined by a set of backhaul reliability levels.

$$S^{\text{as}}(e) \stackrel{P_T/\sigma_n^2 \rightarrow \infty}{=} \Lambda_K \triangleq S^L. \quad (26)$$

⁵This is an approximation in the high SNR region. Especially, this expression is the upper bound on the conditional SER of the square M-QAM [41].

$$R = \frac{1}{\ln(2)} \sum_{k=1}^K (-1)^k \Upsilon \prod_{t=1}^k \left(\frac{s_{qt}}{\ell_t! (\eta_{qt})^{\ell_t}} \right) \left(\bar{l} G_{2,3}^{3,1}(\beta | \begin{smallmatrix} -\bar{l}, 1-\bar{l} \\ 0, -\bar{l}, -\bar{l} \end{smallmatrix}) - \beta G_{2,3}^{3,1}(\beta | \begin{smallmatrix} -1-\bar{l}, -\bar{l} \\ 0, -1-\bar{l}, -1-\bar{l} \end{smallmatrix}) \right). \quad (17)$$

$$R^{\text{as}} = \begin{cases} -\sum_{k=1}^K (-1)^k \Upsilon \prod_{t=1}^k \left(\frac{s_{qt}}{\ell_t! (\eta_{qt})^{\ell_t}} \right) (\beta)^{-\bar{l}} \Gamma(\bar{l}+1) (\psi(\bar{l}+1) - \log(\beta)), & \text{for } \bar{l} = 0, \\ \sum_{k=1}^K (-1)^k \Upsilon \prod_{t=1}^k \left(\frac{s_{qt}}{\ell_t! (\eta_{qt})^{\ell_t}} \right) (\beta)^{-\bar{l}} \Gamma(\bar{l}+1) (\psi(\bar{l}) - \psi(\bar{l}+1)), & \text{for } \bar{l} > 0 \end{cases}. \quad (21)$$

Proof: According to (A.4), we have

$$F_{\lambda}(x) = \prod_{k=1}^K \left(1 - \frac{s_k \Gamma\left(m_k, \frac{m_k \sigma_n^2 x}{P_T E\{|h_k|^2\}}\right)}{\Gamma(m_k)} \right) \\ \approx \prod_{k=1}^K (1 - s_k) \\ \xrightarrow{\frac{P_T}{\sigma_n} \rightarrow \infty}$$

since $\Gamma\left(m_k, \frac{m_k \sigma_n^2 x}{P_T E\{|h_k|^2\}}\right) \xrightarrow{P_T/\sigma_n^2 \rightarrow \infty} \Gamma(m_k)$. Thus, we can have

$$S^L \xrightarrow{\frac{P_T}{\sigma_n} \rightarrow \infty} = S(e) = \prod_{k=1}^K (1 - s_k) = \Lambda_K. \quad (27)$$

This theorem shows that system design parameters such as the signal constellation and Nakagami- m fading severity have no impacts on the ASER limit. However, at the same limit on the ASER, the rate of convergence to Λ_K depends on parameters such as the degrees of transmitter cooperation and Nakagami- m parameter ms . This will be verified by the link-level simulations.

E. Performance of the System with the MRT

Under the assumption that CSI is available at the transmitters, the MRT is employed to maximize the SNR at the receiver. With the use of the MRT, the received signal is given by

$$y = \sum_{k=1}^K \sqrt{P_T} g_k h_k v_k \mathbb{I}_k x + z \quad (28)$$

where $g_k \triangleq \frac{|h_k|^2}{\sum_{k'=1}^K |h_{k'}|^2}$, $v_k \triangleq \frac{h_k^*}{|h_k|}$ is the phase rotation of the channel [42]. Also, we assume that $z \sim \mathcal{CN}(0, \sigma_n^2)$. Then the e-SNR⁶ is computed as follows:

$$\lambda^{\text{MRT}} = \sum_{k=1}^K \mathbb{I}_k \lambda_k^{\text{MRT}} \quad (29)$$

where $\lambda_k^{\text{MRT}} \triangleq \frac{P_T |h_k|^2}{\sigma_n^2}$ is identical to λ_k . After some manipulations, the CDF of λ^{MRT} is derived as follows:

$$F_{\lambda^{\text{MRT}}}(x) = \Lambda_K \left(1 + \sum_{i=1}^{\infty} \sum_{j=1}^k \sum_{m_i} \frac{\Omega_{i,j} (-1)^j}{\Gamma(j)} \gamma_l(j, x/\eta_i) \right) \quad (30)$$

⁶Note that the non-coherent joint transmission [43] results in the same expression for the e-SNR.

where $\widetilde{\Sigma} \triangleq \sum_{k=1}^K \sum_{l_1}^{K-k+1} \sum_{l_2=l_1+1}^{K-k+2} \cdots \sum_{l_k=l_{k-1}+1}^K \left(\prod_{n=1}^k \frac{s_{l_n}}{(1-s_{l_n})} \right)$.

In addition, $\Omega_{i,j}$ is defined by

$$\Omega_{i,j} \triangleq \frac{(-1)^{m_i}}{(\eta_i)^{m_i}} \sum_{X(i,j)} \prod_{k=1, k \neq i}^K \binom{m_k + k_k - 1}{k_k} \\ \frac{(\eta_k)^{k_k}}{(1 - \frac{\eta_k}{\eta_i})^{m_k + k_k}} \times (\eta_i)^j \triangleq c_{i,j} \times (\eta_i)^j \quad (31)$$

where $X(i,j)$ denotes a set of K -tuples satisfying the following condition

$$X(i,j) \triangleq \{(k_1, \dots, k_K) : \sum_{k=1}^K k_k = m_k - j \text{ with } k_i = 0\}.$$

From (30), the PDF of λ^{MRT} is derived as follows:

$$f_{\lambda^{\text{MRT}}}(x) = \Lambda_K \left(\delta(x) + \sum_{i=1}^{\infty} \sum_{j=1}^k \sum_{m_i} \frac{\Omega_{i,j} (-1)^j}{\eta_i \Gamma(j)} x^{j-1} e^{-\frac{x}{\eta_i}} \right) \quad (32)$$

where $\delta(\cdot)$ denotes the Dirac delta function. Note that we can readily derived (30) based on Appendix A, and then (32), so that a detailed derivation is not provided. Since the outage probability at a given threshold θ is a particular value of the CDF of λ^{MRT} , it is given by $O_{\text{out}}^{\text{MRT}}(\theta) = F_{\lambda^{\text{MRT}}}(\theta)$.

Corollary 5: Completely reliable backhubs make the MRT achieve the diversity gain $G_d^{\text{MRT}} = \sum_{k=1}^K m_k$.

Proof: See Appendix G. ■

This Corollary verifies that the proposed SC protocol can achieve the same diversity gain as the MRT under completely reliable backhaul connections.

Similar to the SC-assisted cooperative system, the existence of limits on the outage probability and ASE is inevitable to the MRT-assisted cooperative system with unreliable backhubs. This is provided by the following theorem.

Theorem 6: For Nakagami- m fading channels and unreliable backhaul, the asymptotic outage probability limit and the ASER limit of the MRT-assisted cooperative system are, respectively, given by

$$O_{\text{out}}^{\text{as,MRT}}(\theta) = \Lambda_K \text{ and} \\ S^{\text{as,MRT}}(e) = \Lambda_K \quad (33)$$

which shows that the outage probability limit and the ASER limit are same as those of the SC-assisted cooperative system.

Proof: See Appendix H. ■

From this theorem and Theorem 5, we can verify that only a set of backhaul reliability levels exclusively determines the asymptotic limits on the outage probability and asymptotic ASER of the cooperative system employing either the MRT or SC protocol. Also, the same asymptotic limits on the outage probability and asymptotic ASER are existing for the non-coherent joint transmission system.

IV. SIMULATION RESULTS

In the simulations, we use quadrature phase-shift keying (QPSK), 16-QAM, and 64-QAM for signal constellations. We use a fixed e-SNR threshold $\theta = 0.1$ dB in the computation of the outage probability. Non-identical and identical Nakagami- m fading channels are considered in the simulations. Perfect selection combining is performed in the simulations. The curves obtained via link-level Monte Carlo simulations are denoted by **Sim**, whereas analytically derived curves are denoted by **An**. Limits on asymptotic performance metrics under unreliable backhuls are denoted by $P_{\text{out}}^{\text{as},L}$ and S^L . The performance curves obtained for the system employing the MRT are denoted by **MRT**.

A. Outage Probability

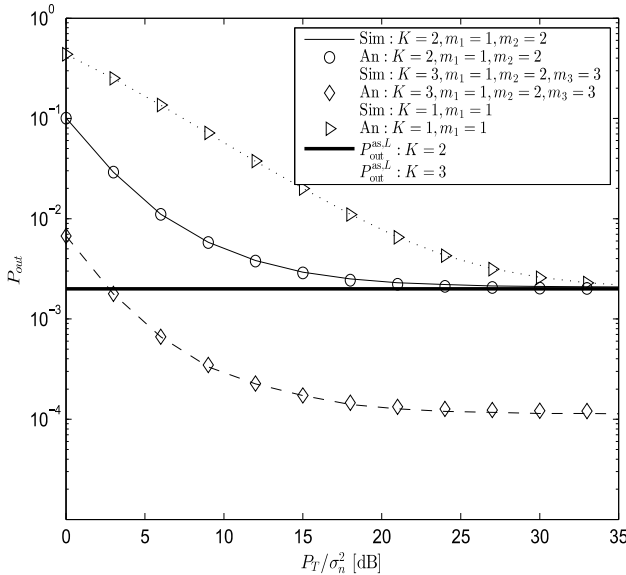


Fig. 2. Outage probability for various levels of backhaul reliability at various degrees of transmitter cooperation and m_k s.

In Fig. 2, we first verify the analytically derived outage probability comparing with that of the simulation. In this figure, we assume $(s_1 = 0.96, s_2 = 0.95)$, and $(s_1 = 0.96, s_2 = 0.95, s_3 = 0.94)$ for $K = 2$ and $K = 3$, respectively, so that we have $\Lambda_2 = 0.002$ and $\Lambda_3 = 1.2 \times 10^{-4}$. For $K = 1$, we assume $s_1 = 0.998$, so that $\Lambda_1 = 0.002$. This figure shows that at the same value of the outage probability limit, $\Lambda_1 = \Lambda_2 = 0.002$, the cooperative system provides a lower outage probability than the non-cooperative system due to an increased receiver e-SNR. We can also see that the

outage probability asymptotically approaches $P_{\text{out}}^{\text{as},L}$ as P_T/σ_n^2 increases.

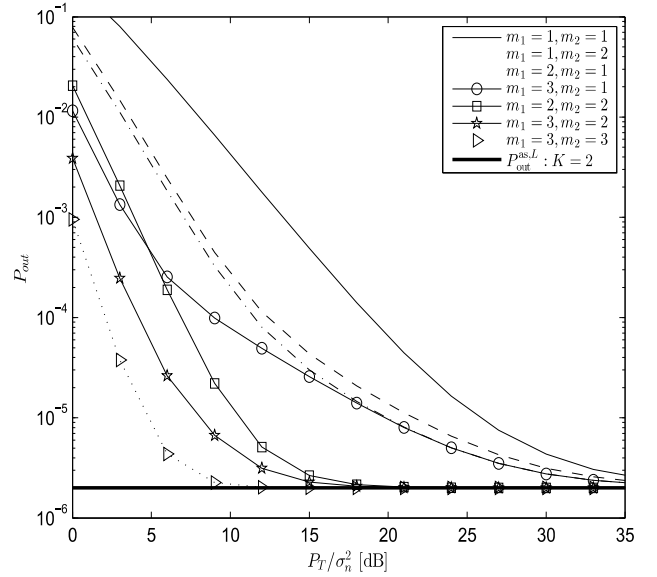


Fig. 3. Outage probability for various values of m_k s at fixed $K = 2$ and $\Lambda_2 = 2 \times 10^{-6}$.

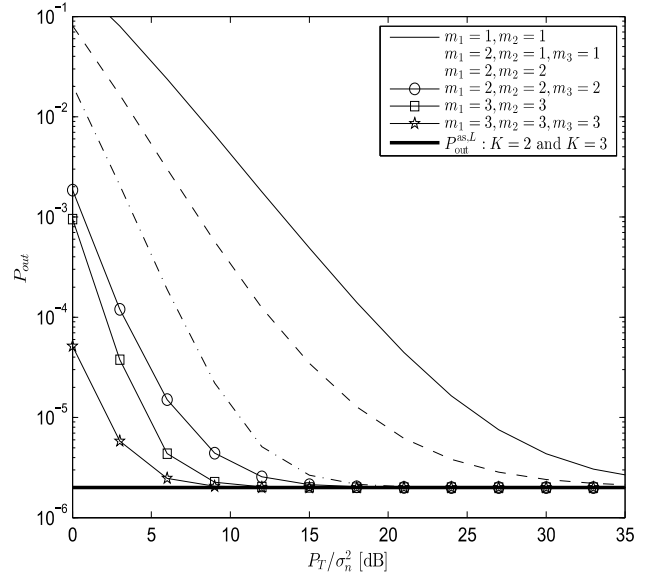


Fig. 4. Outage probability for various values of m_k s at $(K = 2, \Lambda_2 = 2 \times 10^{-6})$ and $(K = 3, \Lambda_3 = 2 \times 10^{-6})$.

To see the effects of various system parameters on the outage probability, we assume $\Lambda_2 = 2 \times 10^{-6}$ and $\Lambda_3 = 2 \times 10^{-6}$ in Figs. 3 and 4. For $K = 2$, we assume $s_1 = 0.999$ and $s_2 = 0.998$, whereas we assume $s_1 = 0.999$, $s_2 = 0.995$, and $s_3 = 0.98$ for $K = 3$ to have the same limit on the outage probability. We can have several observations from Figs. 3 and 4 as follows:

- Two distinctive complementary regions (noise-limited and non-noise-limited) can be observed.
- For $K = 2$, a lower outage probability in the noise-limited region can be achieved with a bigger value of the Nakagami- m parameter. That is, the performance of the considered system in Rayleigh fading is worst due to the largest signal power fluctuation.
- As K or the degrees of transmitter cooperation increases, a lower outage probability is achieved in the noise-limited region in line with Corollary 3. At the same degrees of transmitter cooperation, the rate of convergence to the limit on the outage probability can be seen to be determined by $\min(\{m_k\})$. For example, $(m_1 = 1, m_2 = 1)$ has the same convergence rate as $(m_1 = 2, m_2 = 1)$, $(m_1 = 1, m_2 = 2)$, and $(m_1 = 3, m_2 = 1)$ from Fig. 3, whereas $(m_1 = 2, m_2 = 2)$ and $(m_1 = 3, m_2 = 2)$ approach to Λ_2 faster than the previous case. In the considered scenarios, $(m_1 = 3, m_2 = 3)$ leads to the fastest convergence to Λ_2 due to the biggest $\min(\{m_k\})$. Thus, $\min(\{m_k\})$ is seen to be one of the key factors in determining the rate of convergence to the limit.
- To see how convergence rate behaves in terms of the degrees of transmitter cooperation and the values of fading parameters m_k s, we use the same value of the limit on the outage probability. For $K = 3$, we can see that $(m_1 = 2, m_2 = 1, m_3 = 1)$ has a faster convergence to the limit on the outage probability comparing with $(m_1 = 1, m_2 = 2)$. Similar observation can be observed by comparing $(m_1 = 2, m_2 = 2, m_3 = 2)$ with $(m_1 = 2, m_2 = 2)$. That is, the degrees of transmitter cooperation is another key factor in determining the rate of convergence to the asymptotic outage probability. Thus, the rate of convergence to the asymptotic outage probability can be determined by $K \min(\{m_k\})$.
- This rate of convergence to the asymptotic outage probability also determines the performance of the outage probability in the noise limited region. For example, although $(m_1 = 2, m_2 = 2, m_3 = 2)$ has the same asymptotic outage probability Λ_3 as $(m_1 = 3, m_2 = 3, m_3 = 3)$, $(m_1 = 3, m_2 = 3, m_3 = 3)$ provides a lower outage probability in the noise limited region.

In Fig. 5, we compare the outage probability of the SC-assisted cooperative system with the MRT-assisted cooperative system. Completely reliable and unreliable backhauls are separately considered to investigate the achievable diversity gain promised by two cooperative schemes. Based on the diversity gain derived in Corollary 3 and Corollary 5, we see that the SC-assisted cooperative system has the same diversity gain as the MRT-assisted cooperative system with completely reliable backhauls. By measuring the slope of the curves, we can compute the diversity gain. Since the diversity gain is given by $G_d = \sum_{k=1}^K m_k$, $(m_1 = 2, m_2 = 2)$ results in a higher diversity gain than $(m_1 = 1, m_2 = 2)$. We can also see that the MRT-assisted cooperative system results in a lower outage probability than the SC-assisted cooperative system. At a fixed P_T , we can also observe that the outage probability of these two cooperative systems under unreliable backhauls

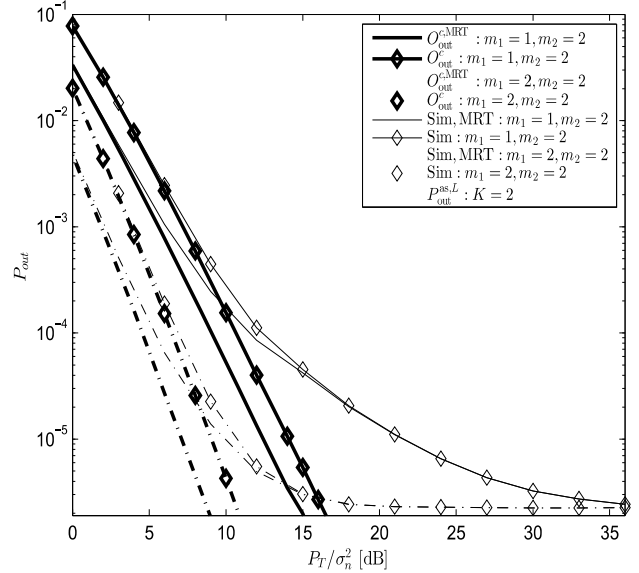


Fig. 5. Outage probability for various values of m_k s at ($K = 2, \Lambda_2 = 2 \times 10^{-6}$).

approaches the outage probability with completely reliable backhauls when σ_n^2 is large, whereas the outage probability approaches the outage limit with imperfect backhauls when σ_n^2 is small.

B. Average Spectral Efficiency

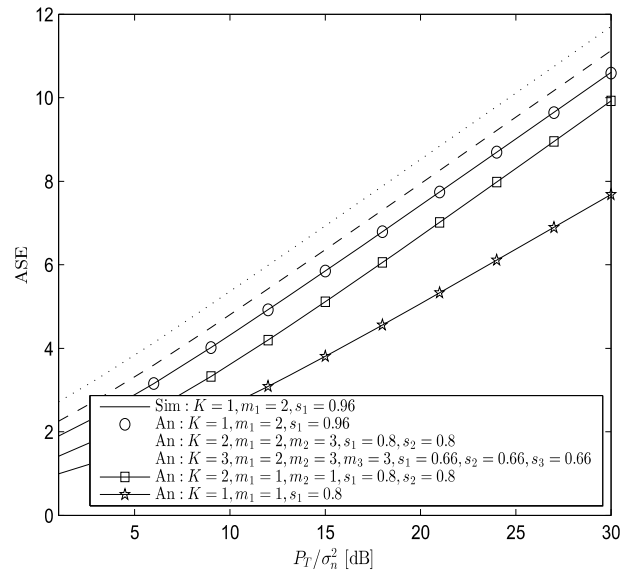


Fig. 6. ASE for various values of K at a fixed outage limit.

In Fig. 6, we first verify the accuracy of our derivation for the analytical ASE comparing with the simulation for $K = 1, m_1 = 2$ at the value of $\Lambda_1 = 0.04$. We can find a good match between them. This figure also shows that at the same value of

the outage limit, $\Lambda_1 = \Lambda_2 = \Lambda_3 = 0.04$, more transmitters in cooperation result in a higher ASE, for example, $(m_1 = 2, \Lambda_1)$ vs. $(m_1 = 2, m_2 = 3, \Lambda_2)$, and $(m_1 = 2, m_2 = 3, \Lambda_2)$ vs. $(m_1 = 2, m_2 = 3, m_3 = 3, \Lambda_3)$.

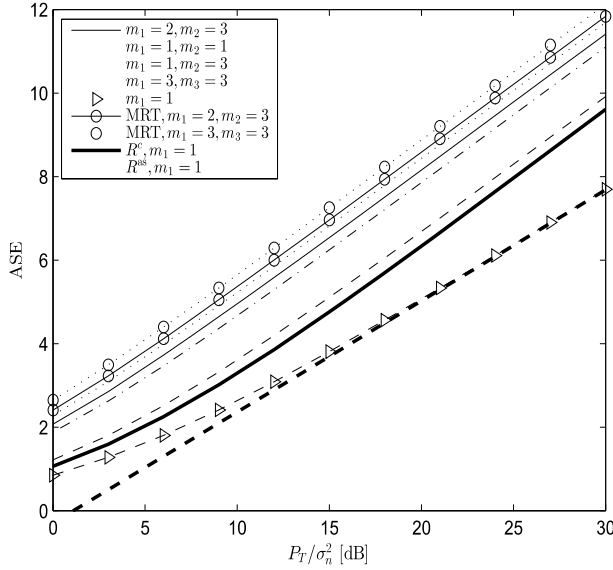


Fig. 7. ASE for various values of m_1 and m_2 at fixed $K = 2$ and $\Lambda_2 = 0.02$.

At a fixed value of $\Lambda_2 = 0.02$, we see the ASE in Fig. 7 for two transmitters with different Nakagami- m parameters. As either of m s increases, a higher ASE can be achieved due to reduced fluctuation of the signal power. Thus, the ASE in Rayleigh fading has the lowest ASE. We also compare the asymptotic ASE, R^{as} , with the simulation in Rayleigh fading. As P_T/σ_n^2 increases, the difference between the asymptotic ASE and the analytical ASE becomes unnoticeable. The analytical ASE is also compared with the ASE of the cooperative system with completely reliable backhails, R^c . It can be observed that as P_T/σ_n^2 increases, the difference between the analytical ASE and R^c increases. From Figs. 6 and 7, we can have a higher ASE as either K or $\sum_{k=1}^K m_k$ increases. Comparing with the SC-assisted cooperative system, the MRT-assisted cooperative system is shown to achieve a higher ASE.

C. Average Symbol Error Rate

In Fig. 8, we first compute ASER of the systems that have the same asymptotic limits on the ASER for different degrees of transmitter cooperation and Nakagami- m parameters. QPSK is used as the signal constellation. In addition, we use a same level of backhaul reliability s , which is determined by $s = 1 - \Lambda_K^{(1/K)}$. At a fixed $\Lambda_1 = \Lambda_2 = 0.05$, a more transmitter cooperation results in a lower ASER in the noise-limited region due to a higher receiver e-SNR, which is promised by the SC protocol. Additionally, $m_1 = 2$ results in a lower ASER in the noise-limited region over $m_1 = 1$ for the non-cooperative system due to a reduced fluctuation of the signal power. For more reliable backhails; for example, $\Lambda_1 = \Lambda_2 = 0.0025$, similar behaviors in the ASER can be

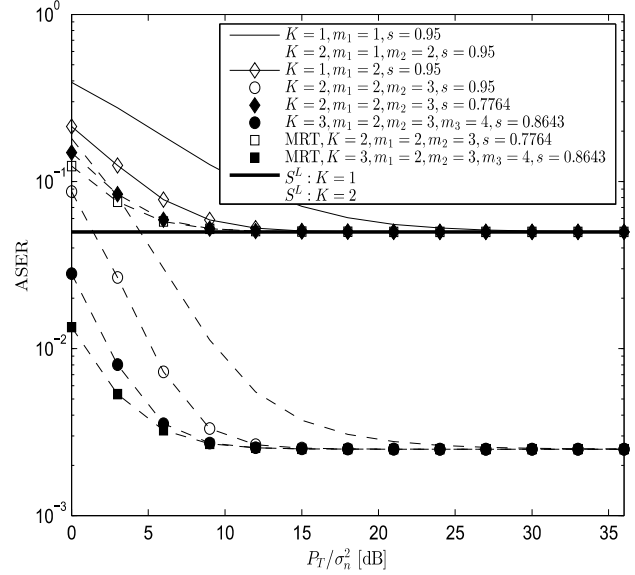


Fig. 8. ASER for various values of K and m_k s at different ASER limits.

observed. We also compare the ASER for the SC-assisted and MRT-assisted cooperative systems. At a fixed P_T , the MRT-assisted cooperative system has a lower ASER than the SC-assisted cooperative system when σ_n^2 is large, whereas the ASER differences become negligible when σ_n^2 is small. In this region, the ASER of two systems depends only on backhaul reliability.

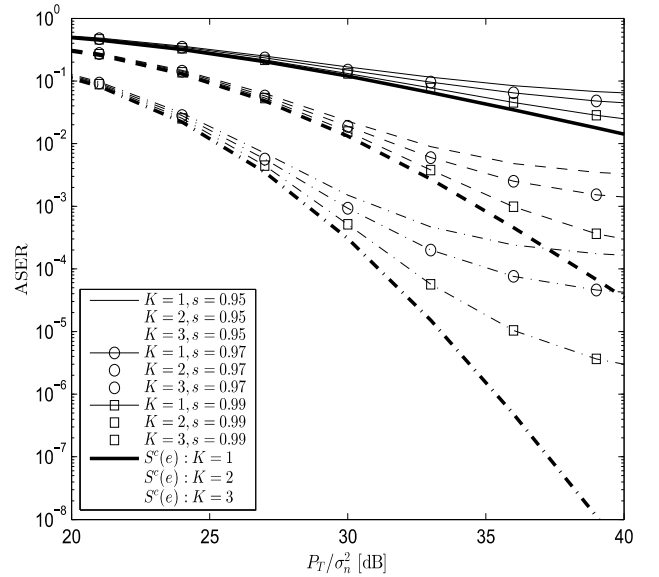


Fig. 9. ASER for various values of K and backhaul reliability.

At fixed Nakagami- m parameters and QPSK signal constellation, the impacts of backhaul reliability and degrees of transmitter cooperation on the ASER of the systems with completely reliable backhails are presented in Fig. 9. We

assume $m_1 = 1$, $m_2 = 2$, and $m_3 = 3$ for this scenario. We can see that the system with completely reliable backhauls can achieve the diversity gain, specified by $\sum_{k=1}^K m_k$. However, the system with unreliable backhaul starts to lose performance as P_T/σ_n^2 increases. Additionally, it can be seen that as backhaul reliability increases, the diversity gain can be maintained up to a higher region of P_T/σ_n^2 . However, in all the cases, unreliable backhauls result in ASER limits exclusively determined by $(1-s)^K$. Thus, at the same degrees of transmitter cooperation, a lower ASER limit can be obtained as backhaul reliability increases. In addition, at the same backhaul reliability, a lower ASER limit can be obtained as a more transmitter cooperation is involved in the system.

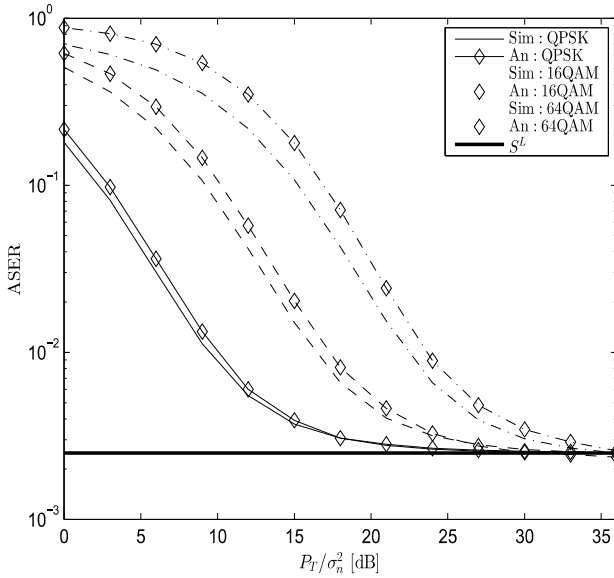


Fig. 10. ASER in different signal constellations.

Fig. 10 illustrates the ASER for different signal constellations. We compare analytical ASERs with their simulation results. As a particular scenario, we assume $K = 2$, $s = 0.95$, $m_1 = 1$ and $m_2 = 2$. For QPSK constellation, the simulation result provides almost perfect match to the analytical result. However, since we use an approximate conditional SER for square M-QAM signal constellations, the link-level simulations result in lower ASERs over the analytical results. However, in the region of high P_T/σ_n^2 , all simulations provide perfect matches to the ASER limit, $\Lambda_2 = 0.0025$. Thus, we can see that the signal constellation only impacts the ASER in the noise-limited region, whereas its impacts are unnoticeable in the asymptotic region where the ASER limit dominates the performance.

V. CONCLUSIONS

In this paper, we have examined the performance of cooperative systems with unreliable backhaul connections. In these systems, the transmitters are connected to the control unit via unreliable wireless backhauls, and the receiver employs the selection combining protocol. We have presented a general

framework for non-identical Nakagami- m fading channels by characterizing the statistics of the e-SNR at the receiver. Based on the derived expression of the e-SNR, closed-form expressions for the outage probability, ASE, and ASER have been derived and validated using link-level simulations. We have verified that the backhaul reliability is a key factor that determines the asymptotic performance limits on the outage probability and the ASER. Furthermore, the conventional diversity gain is not achievable in the non-noise-limited region due to unreliable backhaul links, nevertheless the diversity gain is achievable in the noise-limited region with a limited impact from unreliable backhauls. Under completely reliable backhaul connection, SC-assisted cooperative systems have been shown to achieve the same diversity gain as MRT-assisted cooperative systems.

APPENDIX A: DERIVATION OF THEOREM 1

Let us start from the definition of the random variable λ , which is given by

$$\lambda = \max_{k=1, \dots, K} (\mathbb{I}_k \lambda_k) \quad (\text{A.1})$$

where $\lambda_k \sim \text{Ga}(m_k, \eta_k)$. In (A.1), a particular random variable $\mathbb{I}_k \lambda_k$ has the following PDF

$$f_{\mathbb{I}_k \lambda_k}(x) = (1 - s_k) \delta(x) + \frac{s_k}{\Gamma(m_k) (\eta_k)^{m_k}} x^{m_k-1} e^{-x/\eta_k} \quad (\text{A.2})$$

where $\delta(\cdot)$ denotes the Dirac delta function. In addition, the CDF of $\mathbb{I}_k \lambda_k$ is given by

$$F_{\mathbb{I}_k \lambda_k}(x) = 1 - \frac{s_k \Gamma(m_k, x/\eta_k)}{\Gamma(m_k)}. \quad (\text{A.3})$$

Thus, we can have the CDF of λ as follows:

$$\begin{aligned} F_\lambda(x) &= \prod_{k=1}^K F_{\mathbb{I}_k \lambda_k}(x) \\ &= \prod_{k=1}^K \left(1 - \frac{s_k \Gamma(m_k, x/\eta_k)}{\Gamma(m_k)} \right) \\ &= 1 + \sum_{k=1}^K \sum_{q_1=1}^{K-k+1} \sum_{q_2=q_1+1}^{K-k+2} \cdots \sum_{q_k=q_{k-1}+1}^K (-1)^k \\ &\quad \prod_{t=1}^k \left(\frac{s_{q_t} \Gamma(m_{q_t}, x/\eta_{q_t})}{\Gamma(m_{q_t})} \right). \end{aligned} \quad (\text{A.4})$$

Substituting the series expansions of the upper incomplete gamma function [30, eq. 8.352.2], results in

$$\begin{aligned} F_\lambda(x) &= 1 + \sum_{k=1}^K \sum_{q_1=1}^{K-k+1} \sum_{q_2=q_1+1}^{K-k+2} \cdots \sum_{q_k=q_{k-1}+1}^K (-1)^k \\ &\quad \left(\prod_{t=1}^k s_{q_t} \right) e^{-\sum_{t=1}^k \frac{x}{\eta_{q_t}}} \prod_{t=1}^k \left(\sum_{\ell=0}^{m_{q_t}-1} \frac{x^\ell}{\ell! (\eta_{q_t})^\ell} \right) \\ &= 1 + \sum_{k=1}^K \Upsilon(-1)^k \prod_{t=1}^k \left(\frac{s_{q_t}}{\ell_t! (\eta_{q_t})^{\ell_t}} \right) \\ &\quad e^{-\sum_{t=1}^k \frac{x}{\eta_{q_t}}} x^{\sum_{t=1}^k \ell_t} \end{aligned} \quad (\text{A.5})$$

where we define the summation over all combinations of links and Nakagami- m m values between the transmitters and receiver.

APPENDIX B: DERIVATION OF COROLLARY (3)

For completely reliable backhalls, the asymptotic CDF of λ is given by

$$F_\lambda(x) = \prod_{k=1}^K \left(1 - \frac{\Gamma(m_k, x/\eta_k)}{\Gamma(m_k)} \right) \\ = \prod_{k=1}^K \left(1 - e^{-\frac{m_k \sigma_n^2 x}{P_T E\{|h_k|^2\}}} \sum_{l=0}^{m_k-1} \frac{\left(\frac{m_k \sigma_n^2 x}{P_T E\{|h_k|^2\}} \right)^l}{\Gamma(l+1)} \right). \quad (\text{B.1})$$

At a fixed e-SNR threshold θ , and as $P_T/\sigma_n^2 \rightarrow \infty$, the outage probability is asymptotically given by [44]

$$O_{\text{out}}^{\text{as},c}(\theta) = \prod_{k=1}^K \frac{\left(\frac{\theta m_k}{E\{|h_k|^2\}} \right)^{m_k}}{\Gamma(m_k + 1)} \left(\frac{P_T}{\sigma_n^2} \right)^{-m_k} \\ = C_1 \left(\frac{P_T}{\sigma_n^2} \right)^{-\sum_{k=1}^K m_k} \quad (\text{B.2})$$

which proves (14).

APPENDIX C: PROOF OF THEOREM 2

We use again (A.2) in the computation of the CDF as follows:

$$F_\lambda(x) = \prod_{k=1}^K \left((1 - s_k) + s_k \frac{\gamma_l(m_k, x/\eta_k)}{\Gamma(m_k)} \right) \\ = \prod_{k=1}^K (1 - s_k) \prod_{k=1}^K \left(1 + \frac{s_k}{1 - s_k} \frac{\gamma_l(m_k, x/\eta_k)}{\Gamma(m_k)} \right). \quad (\text{C.1})$$

Substituting the series expansions of the lower incomplete gamma function [30, eq. 8.352.1], (C.1) is equal to (C.2) at the top of the next page. At a given e-SNR threshold θ , $e^{-\frac{m_k \sigma_n^2 \theta}{P_T E\{|h_k|^2\}}} \approx 1$, and K_1 is dominated by the $l = 0$ term as $P_T/\sigma_n^2 \rightarrow \infty$, so that

$$O_{\text{out}}^{\text{as}}(\theta) = \Lambda_K. \quad (\text{C.3})$$

APPENDIX D: PROOF OF THEOREM 3

To solve the integral in (17), we express $\ln(1+x)$ of the integrand in terms of the Meijer G-function according to [28, eq.(07.34.03.0456.01)]:

$$\ln(1+x) = G_{2,2}^{1,2} \left(x \left| \begin{matrix} 1, 1 \\ 1, 0 \end{matrix} \right. \right). \quad (\text{D.1})$$

Using (D.1), the ASE is computed as follows:

$$R = \frac{1}{\ln(2)} \int_0^\infty \ln(1+x) f_\lambda(x) dx \\ = \frac{1}{\ln(2)} \sum_{k=1}^K (-1)^k \Upsilon \prod_{t=1}^k \left(\frac{s_{qt}}{\ell_t! (\eta_{qt})^{\ell_t}} \right) \\ \left(\underbrace{\bar{l} \int_0^\infty e^{-\beta x} x^{\bar{l}-1} G_{2,2}^{1,2} \left(x \left| \begin{matrix} 1, 1 \\ 1, 0 \end{matrix} \right. \right) dx}_{K_2} - \right. \\ \left. \underbrace{\beta \int_0^\infty e^{-\beta x} x^{\bar{l}} G_{2,2}^{1,2} \left(x \left| \begin{matrix} 1, 1 \\ 1, 0 \end{matrix} \right. \right) dx}_{K_3} \right). \quad (\text{D.2})$$

Applying (1), K_2 and K_3 are computed as follows:

$$K_2 = \bar{l}(\beta)^{-(\bar{l})} G_{3,2}^{1,3} \left(\frac{1}{\beta} \left| \begin{matrix} 1 - \bar{l}, 1, 1 \\ 1, 0 \end{matrix} \right. \right) \text{ and} \\ K_3 = \beta(\beta)^{-(\bar{l}+1)} G_{3,2}^{1,3} \left(\frac{1}{\beta} \left| \begin{matrix} -\bar{l}, 1, 1 \\ 1, 0 \end{matrix} \right. \right). \quad (\text{D.3})$$

Using the translation formula of the Meijer G-function [28, eqs. (07.34.17.0011.01) and (07.34.17.0012.01)], K_2 and K_3 are equivalent to the followings:

$$K_2 = \bar{l} G_{2,3}^{3,1} \left(\beta \left| \begin{matrix} -\bar{l}, 1 - \bar{l} \\ 0, -\bar{l}, -\bar{l} \end{matrix} \right. \right) \text{ and} \\ K_3 = \beta G_{2,3}^{3,1} \left(\beta \left| \begin{matrix} -1 - \bar{l}, -\bar{l} \\ 0, -1 - \bar{l}, -1 - \bar{l} \end{matrix} \right. \right). \quad (\text{D.4})$$

Now substituting (D.4) into (D.2), we can derive (17).

APPENDIX E: DERIVATION OF THEOREM 3

According to [39], [40], (22) can be alternatively expressed as follows:

$$S(e) = \int_0^\infty P_e(x|\lambda) f_\lambda(x) dx \\ = \frac{A\sqrt{B}}{\sqrt{2\pi}} \int_0^\infty F_\lambda(t) e^{-Bt} t^{-1/2} dt. \quad (\text{E.1})$$

Using again $F_\lambda(x)$, we can compute the ASER as

$$S(e) = 1 + \sum_{k=1}^K (-1)^k \Upsilon \prod_{t=1}^k \left(\frac{s_{qt}}{\ell_t! (\eta_{qt})^{\ell_t}} \right) \\ \frac{A\sqrt{B}}{\sqrt{2\pi}} \underbrace{\int_0^\infty e^{-(B+\beta)t} t^{\bar{l}-1/2} dt}_{K_4} \quad (\text{E.2})$$

where K_4 is evaluated as

$$K_4 = \Gamma(l+1/2) (\beta+B)^{-(l+1/2)} \quad (\text{E.3})$$

so that we can obtain (24).

$$F_\lambda(x) = \Lambda_K \prod_{k=1}^K \left(1 + \frac{s_k}{1-s_k} \left(1 - e^{-\frac{m_k \sigma_n^2 x}{P_T E\{|h_k|^2\}}} \underbrace{\sum_{l=0}^{m_k-1} \frac{\left(\frac{m_k \sigma_n^2 x}{P_T E\{|h_k|^2\}}\right)^l}{\Gamma(l+1)}}_{K_1} \right) \right). \quad (\text{C.2})$$

APPENDIX F: DERIVATION OF COROLLARY 4

We use again (B.1) for the asymptotic analysis of the ASER. As $P_T/\sigma_n^2 \rightarrow \infty$, it is given that [44]

$$F_\lambda^{\text{as}}(t) = \prod_{k=1}^K \frac{\left(\frac{m_k \sigma_n^2 t}{P_T E\{|h_k|^2\}}\right)^{m_k}}{\Gamma(m_k + 1)}. \quad (\text{F.1})$$

Now replacing $F_\lambda(t)$ with $F_\lambda^{\text{as}}(t)$ in the computation of the ASER, we can have

$$\begin{aligned} S^{\text{as}}(e) &= \frac{A\sqrt{B}}{\sqrt{2\pi}} \prod_{k=1}^K \left(\frac{m_k \sigma_n^2 x}{P_T E\{|h_k|^2\}}\right)^{m_k} \\ &\quad \int_0^\infty \frac{(t)^{m_k-1/2}}{\Gamma(m_k + 1)} e^{-Bt} dt \\ &= \frac{A\sqrt{B}}{\sqrt{2\pi}} \prod_{k=1}^K \left(\frac{m_k \sigma_n^2}{P_T E\{|h_k|^2\}}\right)^{m_k} \frac{\Gamma(m_k + 1/2)}{\Gamma(m_k + 1)} \\ &\quad B^{-(m_k+1/2)} \\ &= C_2 \prod_{k=1}^K \left(\frac{P_T}{\sigma_n^2}\right)^{-m_k} \end{aligned} \quad (\text{F.2})$$

where $C_2 \triangleq \frac{A\sqrt{B}}{\sqrt{2\pi}} \prod_{k=1}^K \left(\frac{m_k \sigma_n^2}{P_T E\{|h_k|^2\}}\right)^{m_k} \frac{\Gamma(m_k+1/2)}{\Gamma(m_k+1)} \left(\frac{P_T}{\sigma_n^2}\right)^{-m_k}$. Thus, the asymptotic diversity gain can be obtained as $G_{d,\text{ASER}} = \sum_{k=1}^K m_k$.

APPENDIX G: DERIVATION OF COROLLARY 5

In the high SNR region, we can approximate the outage probability as

$$\begin{aligned} O_{\text{out}}^{\text{as,MRT}}(\theta) &\underset{\frac{P_T}{\sigma_n^2} \rightarrow \infty}{\approx} \left(\widetilde{\sum}_{i=1}^k \sum_{j=1}^{m_i} \frac{\Omega_{i,j} (-1)^j}{\Gamma(j+1)} \left(\frac{\theta}{\eta_{l_i}}\right)^j \right) \\ &\approx C_3 \sum_{k=1}^K \sum_{l_1=1}^{K-k+1} \sum_{l_2=l_1+1}^{K-k+2} \dots \sum_{l_k=l_{k-1}+1}^K \prod_{n=1}^k \left(\frac{P_T}{\theta \sigma_n^2}\right)^{m_{l_n}} \\ &\approx \prod_{k=1}^K C_{3,k} \left(\frac{P_T}{\sigma_n^2}\right)^{-m_k} = \left(\prod_{k=1}^K C_{3,k}\right) \left(\frac{P_T}{\sigma_n^2}\right)^{-\sum_{k=1}^K m_k} \end{aligned} \quad (\text{G.1})$$

where C_3 and $C_{3,k}$ are constants. Note that we use an approximation of the incomplete gamma function [44].

APPENDIX H: DERIVATION OF THEOREM 6

Based on the derivations used in Appendix G, we can have

$$\begin{aligned} O_{\text{out}}^{\text{as,MRT}}(\theta) &\underset{\frac{P_T}{\sigma_n^2} \rightarrow \infty}{\approx} \Lambda_K \left(1 + \left(\prod_{k=1}^K C_{3,k} \right) \left(\frac{P_T}{\sigma_n^2}\right)^{-\sum_{k=1}^K m_k} \right) \\ &= \Lambda_K. \end{aligned} \quad (\text{H.1})$$

Also, we can derive the ASER of the MRT-assisted cooperative system for QPSK signal constellation in (H.2) at the top of the next page. A constant term Λ_K becomes dominating as the second term in the right hand side of (H.2) is diminishing which is noticeable as $\frac{P_T}{\sigma_n^2}$ increases. Thus, the ASER performance is limited by Λ_K . For other signal constellations, we can derive the same limit.

REFERENCES

- [1] J. Andrews, S. Buzzi, W. Choi, S. Hanly, A. Lozano, A. Soong, and J. Zhang, "What will 5G be?" *IEEE J. Sel. Areas Commun.*, vol. 32, no. 6, p. 10651082, Jun. 2014.
- [2] J. Andrews, "Seven ways that hetnets are a cellular paradigm shift," *IEEE Commun. Mag.*, vol. 51, no. 3, pp. 136–144, Mar. 2013.
- [3] Z. Mayer, J. Li, A. Papadogiannis, and T. Svensson, "On the impact of control channel reliability on coordinated multi-point transmission," *EURASIP Journal on Wireless Communications and Networking*, vol. 2014:28, pp. 1–16, 2014.
- [4] O. Tipmongkolsilp, S. Zaghoul, and A. Jukan, "The evolution of cellular backhaul technologies: Current issues and future trends," *IEEE Commun. Surveys Tuts.*, vol. 13, pp. 97–113, 2012.
- [5] P. Xia, C.-H. Liu, and J. G. Andrews, "Downlink coordinated multi-point with overhead modeling in heterogeneous cellular networks," *IEEE Trans. Wireless Commun.*, vol. 12, no. 8, pp. 4025–4037, Aug. 2013.
- [6] S.-H. Park, O. Simeone, O. Sahin, and S. Shamai, "Robust and efficient distributed compression for cloud radio access networks," *IEEE Trans. Veh. Technol.*, vol. 62, no. 2, pp. 692–703, Feb. 2013.
- [7] F. Pantisano, M. Bennis, W. Saad, M. Debbah, and M. Latva-aho, "On the impact of heterogeneous backhuls on coordinated multipoint transmission in femtocell networks," in *Proc. IEEE Int. Conf. Commun.*, Ottawa, Canada, Jun. 2012, pp. 5064–5069.
- [8] S. Simeone, O. Somekh, E. Erkip, H. V. Poor, and S. Shamai, "Robust communication via decentralized processing with unreliable backhaul links," *IEEE Trans. Inf. Theory*, vol. 57, pp. 4187–4201, Jul. 2011.
- [9] D. Torrieri and M. C. Valenti, "The outage probability of a finite Ad Hoc network in Nakagami fading," *IEEE Trans. Commun.*, vol. 60, pp. 2960–2970, Dec. 2012.
- [10] J. Guo, S. Durrani, and X. Zhou, "Outage probability in arbitrarily-shaped finite wireless networks," *IEEE Trans. Commun.*, vol. 62, pp. 699–712, Feb. 2014.
- [11] Y. Li, X. Wang, S. Zhou, and S. Alshomrani, "Uplink coordinated multi-point reception with limited backhaul via cooperative group decoding," *IEEE Trans. Wireless Commun.*, vol. 13, no. 6, pp. 3017–3030, Jun. 2014.
- [12] J. Du, M. Xiao, M. Skoglund, and M. Medard, "Wireless multicast relay networks with limited-rate source-conferencing," *IEEE J. Sel. Areas Commun.*, vol. 31, no. 8, pp. 1390–1401, Aug. 2013.
- [13] J. Du, M. Xiao, and M. Skoglund, "Cooperative network coding strategies for wireless relay networks with backhaul," *IEEE Trans. Commun.*, vol. 60, pp. 2502–2514, Sep. 2011.
- [14] H. Phan, F. Zheng, and M. Fitch, "Wireless backhaul networks with precoding complex field network coding," *IEEE Commun. Lett.*, 2015, under publication.
- [15] P. de Kerret, R. Fritzsche, D. Gesbert, and U. Salim. (2014) Robust precoding for network MIMO with hierarchical CSIT. [Online]. Available: <http://arxiv.org/abs/1406.7708>
- [16] Z. Chen, J. Yuan, and B. Vucetic, "Analysis of transmit antenna selection/maximal-ratio combining in Rayleigh fading channels," *IEEE Trans. Veh. Technol.*, vol. 54, no. 4, pp. 1312–1321, July 2005.
- [17] N. Yang, P. L. Yeoh, M. Elkashlan, R. Schober, and I. B. Collings, "Transmit antenna selection for security enhancement in MIMO wiretap channels," *IEEE Trans. Commun.*, vol. 61, no. 1, pp. 144–154, Jan. 2013.

$$S^{\text{MRT}}(\epsilon) = \Lambda_K \left(1 + \sum_{i=1}^k \sum_{j=1}^{m_i} \frac{c_{i,j}(-1)^j}{\Gamma(j)} \frac{1}{\sqrt{\pi}} \left(\frac{1}{\eta_i} \right)^{-j} G_{2,2}^{2,1} \left(\sin^2(\pi/4)\eta_i \middle| \begin{matrix} 1-j, 1 \\ 0, 1/2 \end{matrix} \right) \right). \quad (\text{H.2})$$

- [18] H. Zhang, A. F. Molish, and J. Zhang, "Applying antenna selection in WLANs for achieving broadband multimedia communications," *IEEE Trans. Broadcast.*, vol. 52, no. 4, pp. 475–482, Dec. 2006.
- [19] Q. Li, X. Lin, J. Zhang, and W. Roh, "Advancement of MIMO technology in WiMAX: From IEEE 802.16d/e/j to 802.16m," *IEEE Commun. Mag.*, vol. 47, no. 6, pp. 100–107, June 2009.
- [20] Institute of Communications and Navigation, "Final report of the maritime traffic engineering projects: E-navigation integrity," 2015. [Online]. Available: [http://www.dlr.de/kn/en/Portaldata/27/Resources/dokumente/04-abteilungen-nas/MVT-Final-Report\(Final\).pdf](http://www.dlr.de/kn/en/Portaldata/27/Resources/dokumente/04-abteilungen-nas/MVT-Final-Report(Final).pdf)
- [21] T. A. Khan, P. Orlik, K. J. Kim, and R. W. Heath, "Performance analysis of cooperative wireless networks with unreliable backhaul links," *IEEE Commun. Lett.*, vol. 19, no. 8, pp. 1386–1389, Aug. 2015.
- [22] M. O. Pun, V. Koivunen, and H. V. Poor, "Performance analysis of joint opportunistic scheduling and receiver design for MIMO-SDMA downlink systems," *IEEE Trans. Commun.*, vol. 59, no. 1, pp. 268–280, 2011.
- [23] K. J. Kim and T. A. Tsiftsis, "Performance analysis of QRD-based cyclically prefixed single-carrier transmissions with opportunistic scheduling," *IEEE Trans. Veh. Technol.*, vol. 60, no. 1, pp. 328–333, Jan. 2011.
- [24] K. J. Kim, T. Q. Duong, and X.-N. Tran, "Performance analysis of cognitive spectrum-sharing single-carrier systems with relay selection," *IEEE Trans. Signal Process.*, vol. 60, no. 12, pp. 6435–6449, Dec. 2012.
- [25] I. Krikidis, J. Thompson, S. McLaughlin, and N. Goertz, "Amplify-and-forward with partial relay selection," *IEEE Commun. Lett.*, vol. 12, pp. 235–237, Apr. 2008.
- [26] K. J. Kim and T. A. Tsiftsis, "On the performance of cyclic prefix-based single-carrier cooperative diversity systems with best relay selection," *IEEE Trans. Wireless Commun.*, vol. 10, no. 4, pp. 1269–1279, Apr. 2011.
- [27] M. Xia, C. Xing, and S. Aissa, "Exact performance analysis of dual-hop semi-blind AF relaying over arbitrary Nakagami- m fading channels," *IEEE Trans. Wireless Commun.*, vol. 10, no. 10, pp. 3449–3459, Oct. 2011.
- [28] The Wolfman functions site. Wolfman research inc. [Online]. Available: <http://functions.wolfman.com>
- [29] A. P. Prudnikov, Y. A. Brychkov, and O. I. Marichev, *Integral and Series. Vol. 3: More Special Functions*, 3rd ed. London: Gordon and Breach, 1992.
- [30] I. S. Gradshteyn and I. M. Ryzhik, *Table of Integrals, Series, and Products*. New York: Academic Press, 2007.
- [31] T. K. Y. Lo, "Maximum ratio transmission," *IEEE Trans. Commun.*, vol. 47, no. 10, pp. 1458–1461, Oct. 1999.
- [32] J. K. Cavers, "Single-user and multiuser adaptive maximal ratio transmission for Rayleigh channels," *IEEE Trans. Veh. Technol.*, vol. 49, no. 6, pp. 2043–2050, Nov. 2000.
- [33] T. A. Tsiftsis, G. K. Karagiannidis, N. C. Sagias, and S. A. Kotsopoulos, "Performance of MRC diversity receivers over correlated nakagami- m fading channels," in *Proc. Communication Systems, Networks and Digital Signal Processing*, Patras, Greece, Jul. 2006, pp. 84–88.
- [34] A. Maaref and R. Annavajjala, "The gamma variate with random shape parameter and some applications," *IEEE Commun. Lett.*, vol. 12, pp. 1146–1148, Dec. 2011.
- [35] J. M. Romero-Jerez and A. J. Goldsmith, "Receive antenna array strategies in fading and interference: An outage probability comparison," *IEEE Trans. Wireless Commun.*, vol. 7, no. 3, pp. 920–932, Mar. 2008.
- [36] H. Yu, I.-H. Lee, and G. L. Stuber, "Outage probability of decode-and-forward cooperative relaying systems with co-channel interference," *IEEE Trans. Wireless Commun.*, vol. 11, no. 1, pp. 266–274, Jan. 2011.
- [37] K. J. Kim, T. Q. Duong, M. ElKashlan, P. L. Yeoh, H. V. Poor, and M. H. Lee, "Spectrum sharing single-carrier in the presence of multiple licensed receivers," *IEEE Trans. Wireless Commun.*, vol. 12, pp. 5223–5235, Oct. 2013.
- [38] N. C. Sagias, G. S. Tombras, and G. K. Karagiannidis, "New results for the Shannon channel capacity in generalized fading channels," *IEEE Commun. Lett.*, vol. 9, no. 2, pp. 97–99, Feb. 2005.
- [39] H. A. Suraweera, P. J. Smith, and M. Shafi, "Capacity limits and performance analysis of cognitive radio with imperfect channel knowledge," *IEEE Trans. Veh. Technol.*, vol. 59, pp. 1811–1822, May 2010.
- [40] G. Karagiannidis, N. Sagias, and T. Tsiftsis, "Closed-form statistics for the sum of squared Nakagami- m variates and its applications," *IEEE Trans. Commun.*, vol. 54, no. 8, pp. 1353–1359, Aug. 2006.
- [41] M. K. Simon and M. S. Alouini, *Digital Communication Over Fading Channels: A Unified Approach to Performance Analysis*, 2nd ed. New York, NY: Wiley, 2005.
- [42] W. Peng, Y. Li, M. Ju, P. Huang, G. Tan, and D. Jiang, "Outage and capacity performance evaluation of distributed MIMO systems over a composite fading channel," *Mathematical Problems in Engineering*, vol. 2014, no. Article ID 510423, pp. 1–11, 2014.
- [43] R. Tanbourgi, S. Singh, J. G. Andrew, and F. K. Jondral, "A tractable model for non-coherent joint-transmission base station cooperation," *IEEE Trans. Wireless Commun.*, vol. 13, no. 9, pp. 4959–4973, Sep. 2014.
- [44] C. Zhong, T. Patnarajah, and K.-K. Wong, "Outage analysis of decode-and-forward cognitive dual-hop systems with the interference constraint in Nakagami- m fading channels," *IEEE Trans. Veh. Technol.*, vol. 60, pp. 2875–2879, Jul. 2011.



Kyeong Jin Kim (SM'11) received the M.S. degree from Korea Advanced Institute of Science and Technology (KAIST), Daejeon, South Korea, in 1991, and the M.S. and Ph.D. degrees in electrical and computer engineering from the University of California, Santa Barbara, Santa Barbara, CA, USA in 2000. From 1991 to 1995, he was a Research Engineer with the Video Research Center of Daewoo Electronics, Ltd., South Korea. In 1997, he joined the Data Transmission and Networking Laboratory, University of California, Santa Barbara.

After receiving his degrees, he joined the Nokia research center (NRC) and Nokia Inc., Dallas, TX, USA, as a Senior Research Engineer, where he was, from 2005 to 2009, an L1 specialist. During 2010–2011, he was an Invited Professor with Inha University, Incheon, South Korea. Since 2012, he has been working as a Senior Principal Research Staff in the Mitsubishi Electric Research Laboratories (MERL), Cambridge, MA. His research interests include transceiver design, resource management, scheduling in the cooperative wireless communications systems, cooperative spectrum sharing system, physical layer secrecy system, and device-to-device communications.

Dr. Kim currently serves as an Editor for the IEEE COMMUNICATIONS LETTERS and *International Journal of Antennas and Propagation*. He also served as a Guest Editor for the *EURASIP Journal on Wireless Communications and Networking*: Special Issue on "Cooperative Cognitive Networks" and *IET Communications*: Special Issue on "Secure Physical Layer Communications". Since 2013, he has served as the TPC Chair for the IEEE GLOBECOM Workshop on Trusted Communications with Physical Layer Security.



Talha Ahmed Khan (S'10) graduated with a B.Sc. in electrical engineering from University of Engineering and Technology Lahore, Pakistan. He received the M.S.E. degree in electrical and computer engineering from The University of Texas at Austin, where he is currently working towards his Ph.D. degree. His research interests include wireless communications, stochastic geometry applications, millimeter wave communications, and energy harvesting. He has held internship positions at Broadcom in 2013, and at Mitsubishi Electric Research Labs in 2014.



Philip V. Orlik (SM'97) was born in New York, NY in 1972. He received the B.E. degree in 1994 and the M.S. degree in 1997 both from the State University of New York at Stony Brook. In 1999 he earned his Ph. D. in electrical engineering also from SUNY Stony Brook.

In 2000 he joined Mitsubishi Electric Research Laboratories Inc. located in Cambridge, MA where he is currently the Team Leader of the Mobile Systems Group. His primary research focus is on advanced wireless and mobile communications, sensor networks, ad hoc networking and UWB. Other research interests include vehicular/car-to-car communications, mobility modeling, performance analysis, and queuing theory.